Proposal
Polarized Proton Acceleration at J-PARC

November 30, 2007

M. Bai[1], M. Brooks[5], J. Chiba[11], N. Doshita[12], Y. Fukao[7], Y. Goto[7,8†], M. Grosse Perdekamp[2], K. Hatanaka[6], H. Huang[1], K. Imai[4], T. Iwata[12], S. Ishimoto[3], X. Jiang[5], K. Kondo[12], G. Kunde[5], K. Kurita[9], M. J. Leitch[5], M. X. Liu[5], A. U. Luccio[1], P. L. McGaughey[5], A. Molodojentsev[3], C. Ohmori[3], J.-C. Peng[2], T. Roser[1], N. Saito[3], H. Sato[3†], S. Sawada[3], R. Seidl[2], T.-A. Shibata[10], J. Takano[3], A. Taketani[7,8], M. Togawa[8], and A. Zelenski[1]

[1] *Brookhaven National Laboratory, Upton, NY 11973, USA*
[2] *University of Illinois at Urbana-Champaign, Urbana, Illinois 61801, USA*
[3] *KEK, High Energy Accelerator Research Organization, Tsukuba, Ibaraki 305-0801, Japan*
[4] *Kyoto University, Kyoto 606-8502, Japan*
[5] *Los Alamos National Laboratory, Los Alamos, NM 87545, USA*
[6] *Research Center for Nuclear Physics, Osaka University, Ibaraki, Osaka 567-0047, Japan*
[7] *RIKEN, Institute of Physical and Chemical Research, Wako, Saitama 351-0198, Japan*
[8] *RIKEN BNL Research Center, Brookhaven National Laboratory, Upton, NY 11973, USA*
[9] *Rikkyo University, Tokyo 171-8501, Japan*
[10] *Tokyo Institute of Technology, Tokyo 152-8551, Japan*
[11] *Tokyo University of Science, Noda, Chiba 278-8510, Japan*
[12] *Yamagata University, Yamagata 990-8560, Japan*

[†]Contact persons: Y. Goto (goto@bnl.gov) and H. Sato (hikaru.sato@kek.jp).

Abstract

We propose to make the J-PARC facility allow acceleration of polarized proton beams to 30-50 GeV for experiments using this primary beam. We have studied the feasibility of polarized proton acceleration at J-PARC consisting of a 400 MeV linac, a 3 GeV rapid cycling synchrotron (RCS) and a 50 GeV synchrotron (MR). We show how the polarization of the beam can be preserved using an rf dipole in the RCS and two superconducting partial helical Siberian snakes in the MR. As a main physics case, polarized Drell-Yan measurement which has never been done before is described. It gives us valuable new experimental data of the polarized proton structures, e.g. flavor structure of the sea-quark polarization, orbital angular momentum and transversity of quarks inside the proton. The polarized proton acceleration at J-PARC will provide a new and unique tool to study the nucleon structure and hadron interactions based on QCD.

Contents

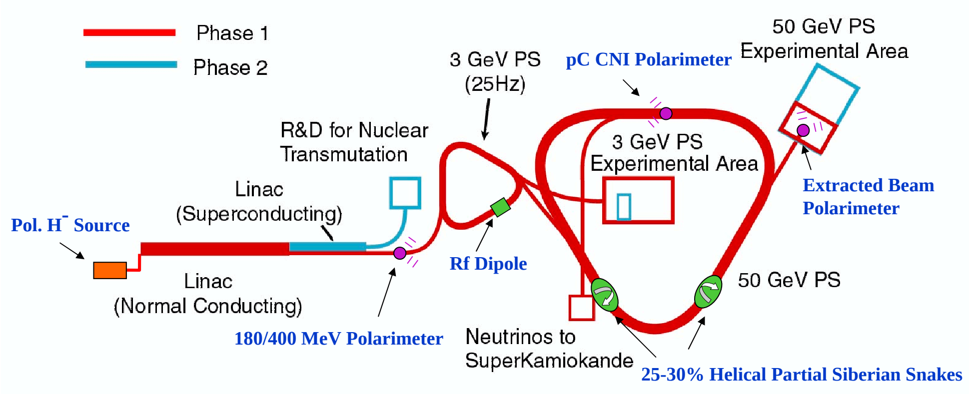

Figure 1: Layout of J-PARC accelerator complex and the hardware needed for polarized beam acceleration.

1 Introduction

1.1 J-PARC Facility

J-PARC facility will allow acceleration of polarized proton beams to 30-50 GeV with some modifications for experiments using this primary beam. The modifications would consist of the addition of a polarized H^- source, an rf dipole in the 3 GeV Rapid Cycling Synchrotron (RCS) and two strong superconducting partial Siberian snakes in the 50 GeV Main Ring (MR). In addition, several external and internal polarimeters are needed for commissioning and operation of polarized proton acceleration. Fig. 1 shows the layout of J-PARC with the items needed for polarized proton acceleration highlighted.[1] The proposed scheme for the acceleration of polarized protons is based on the successful experience of accelerating polarized protons to 25 GeV at the Brookhaven AGS [2, 3], which is very similar to the J-PARC complex.

The required beam bunch parameters that allow the acceleration of polarized protons to 50 GeV are a normalized 95% emittance of $10\pi\mu$m and 0.3 eVs longitudinal emittance. With the present available source intensity of 10^{12} H^- for a 0.5 ms pulse it is easily possible to produce a bunch intensity of 2×10^{11} protons for a single bunch in the RCS.

We propose to make the J-PARC facility allow acceleration of polarized proton beams to 30-50 GeV for experiments using this primary beam. As a main physics case, polarized Drell-Yan measurement by the dimuon experiment which has been proposed [4] is described in the following sections. The polarized proton acceleration at J-PARC will provide a new and unique tool to study the nucleon structure and hadron interactions based on QCD.

1.2 Spin Physics

Although the spin of the nucleon is one of the most fundamental property of the nucleon, it is not understood from the inner structure point of view. In order to understand the inner structure of the nucleon, methods of approach based on perturbative QCD have been well established. The spin structure of the nucleon will give a fundamental understanding of the nucleon structure, and test and understand QCD.

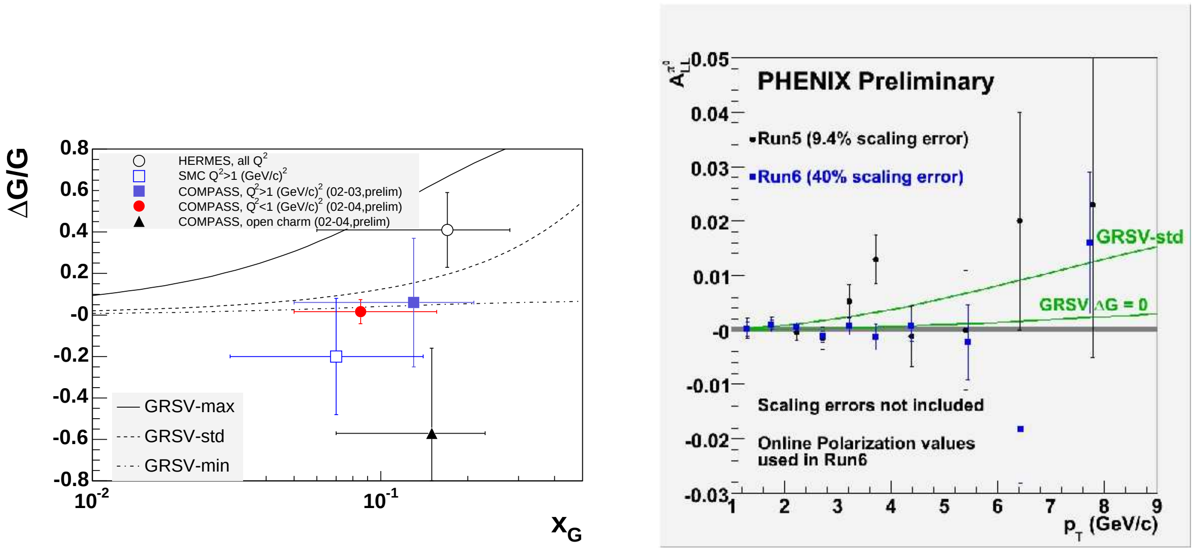

Figure 2: Left: The gluon polarization obtained by COMPASS from high-p_T hadron pairs and open charm production, compared to SMC and HERMES determinations from high-p_T hadron pairs. Right: The double helicity asymmetry in the inclusive π^0 production measured by PHENIX at midrapidity in polarized $p+p$ collisions.

Since the EMC experiment at CERN [5] showed that the quark spin carries only a small portion of the nucleon spin 1/2, it has been one of the biggest issues in the high-energy hadron physics to know what is the origin of the nucleon spin. The nucleon spin is described by:

$$\frac{1}{2} = \frac{1}{2}\Delta\Sigma + \Delta G + L_q + L_g.$$

Contributions other than that from the quark spin ($\Delta\Sigma$) come from the gluon spin (ΔG) and the orbital angular momentum of quarks and gluons ($L_q + L_g$).

In polarized deep-inelastic scattering (DIS) experiments, the contribution of the gluon spin is calculated by the scaling violation property of the Q^2 evolution of parton distributions. SMC experiment at CERN [6] showed ΔG is $0.99^{+1.17}_{-0.31}(\mathrm{stat})^{+0.42}_{-0.22}(\mathrm{syst})^{+1.43}_{-0.45}(\mathrm{th})$ at $Q^2 = 1$ GeV^2, and E155 experiment at SLAC [7] showed it is 1.6±0.8(stat)±1.1(syst) at $Q^2 = 5$ GeV^2. Although the determination of ΔG using this method means a success of the perturbative QCD, it is an indirect way to measure ΔG and the sensitivity is low because the Q^2 coverage of the experimental data is limited.

One direct way is a semi-inclusive asymmetry measurement of high-p_T hadron pair or open-charm production of the polarized DIS experiment. COMPASS experiment at CERN [8] and HERMES experiment at DESY [9] have showed a small gluon polarization by comparing with theoretical GRSV curves with ΔG assumptions.[10, 11] as shown in the left panel of Fig. 2. Another direct way is a double helicity asymmetry (A_{LL}) measurement of polarized hadron collisions:

$$A_{LL} = \frac{\sigma_{++} - \sigma_{+-}}{\sigma_{++} + \sigma_{+-}}$$

where $\sigma_{++}(\sigma_{+-})$ is the cross section of the reaction when two colliding particles have the same (opposite) helicity. Two clear channels are direct photon production and heavy-flavor production. Polarized proton collision experiments at RHIC of BNL have showed

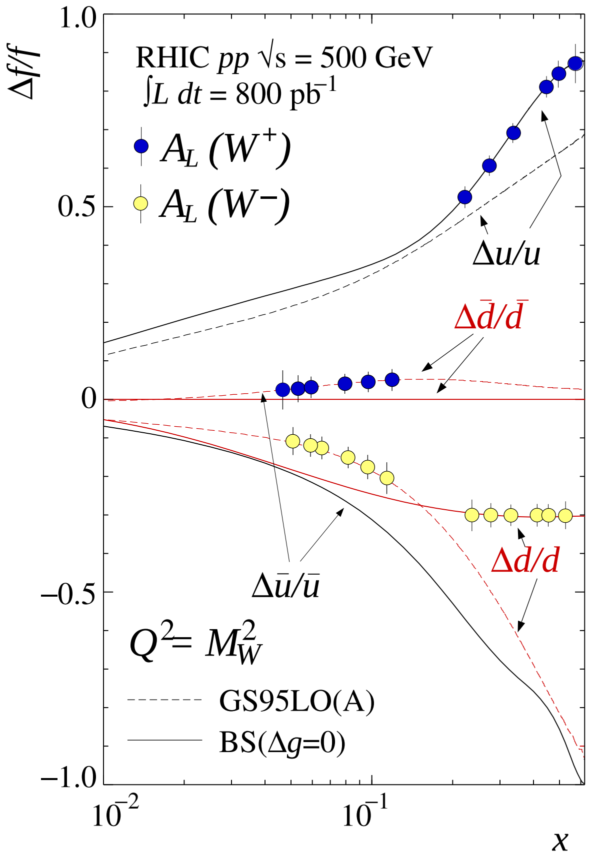

Figure 3: Flavor-sorted sea-quark polarization measurement expected by the weak-boson measurement at RHIC/PHENIX with 500-GeV polarized proton collisions.

their first A_{LL} results of pion and jet production.[12, 13] The A_{LL} measurement of neutral pion production in the PHENIX experiment excludes GRSV standard ΔG scenario which corresponds to $\Delta G = 0.4$ at $Q^2 = 1$ (GeV/c^2)^2, and prefer $\Delta G < 0.3$ at the 3-σ level. From these results, the sum of quark-spin contribution and gluon-spin contribution favors smaller than 1/2. The orbital angular momentum measurements should be developed for the final solution.

To restrict the quark and gluon contribution to the nucleon spin with high precision, it is also important to know the flavor-sorted sea-quark contribution to the nucleon spin directly. Because the Q^2 evolution of the quark and gluon distribution mixes them, uncertainties of the flavor-sorted sea-quark distribution propagate to uncertainties of the quark and gluon distributions. Figure 3 shows a flavor-sorted sea-quark polarization measurement expected by the weak-boson measurement at RHIC/PHENIX with 500-GeV polarized proton collisions in the future. From the parity-violating asymmetry (A_L) measurement of the weak boson, the flavor-sorted sea-quark polarization will be determined by selecting the rapidity region. Polarized Drell-Yan experiment will also provide the flavor-sorted sea-quark distribution, $\Delta\bar{u} - \Delta\bar{d}$ which will be discussed later.

In hadron experiments there is no clear way how to measure L. We have just hints from previous hadron experiments. In the Fermilab E704 experiment which is a fixed-target experiment with 200-GeV polarized proton and antiproton beams, it was observed that there is a large transverse single-spin asymmetry (SSA), or left–right asymmetry A_N:

$$A_N = \frac{\sigma_L - \sigma_R}{\sigma_L + \sigma_R}$$

in pion production in the forward rapidity region.[14] In the naive picture of the QCD, A_N was estimated by $m_q/\sqrt{s}$ and very small. To explain this large A_N, many theoretical explanations are available now, Sivers effect, higher-twist effect, and Collins effect (combined with the transversity distribution).[15] The Sivers effect [16] and the higher-twist effect [17] are related to emitted gluons from initial-state hadron and correlation with gluons inside the hadron, and these effects are related to the transverse motion, or orbital angular motion, of partons inside the hadron.

It is important now to identify contribution of each theoretical mechanism and combine these mechanisms each other. In order to disentangle these effects, many experimental data have been taken and many future experiments are planned. One of the most clear measurements is a Drell-Yan measurement at the hadron experimental facility. The Drell-Yan process is not affected by the final-state and free from Collins effect. Another method is A_N measurements of open charm production (D-meson, etc.) or bounded charm production (J/ψ, etc.) which are also free from the final-state effect.

2 Physics case

2.1 J-PARC Dimuon Experiment

We have proposed the construction of a spectrometer at J-PARC designed for the detection of high-mass dimuons produced in the interactions of 50 GeV primary proton beams with various targets. [4] Through the detections of the Drell-Yan events, a broad physics program addressing various issues in QCD can be pursued. Unique measurements of the nucleon sea-quark flavor asymmetry and the antiquark contents in nuclei can be performed over the large Bjorken-x region of $0.25 < x < 0.6$. A rich program of spin-dependent structure function physics can be carried out through the measurements of unpolarized, singly polarized, and doubly polarized Drell-Yan processes. The construction and operation of this high-mass high-rate dimuon spectrometer at J-PARC will provide a unique tool to study quark nuclear physics.

The proton-induced Drell-Yan process provides a means to probe the flavor asymmetry of the nucleon sea. An important advantage of the Drell-Yan process is that the x dependence of $\bar{d}/\bar{u}$ can be determined. The Fermilab E866 experiment measured the Drell-Yan muon pairs from 800-GeV/c protons interacting with liquid deuterium and hydrogen targets.[18] Values for $\bar{d}/\bar{u}$ were extracted by the E866 collaboration over the region $0.02 < x < 0.345$.

The experimental apparatus is very similar to the one used in a series of experiment at Fermilab (E605, E772, E789, E866, and E906). Just after the experimental target, a large dipole magnet is located in order to focus the high momentum muons and defocus low momentum muons. A copper beam dump and hadron absorbers are inserted in the first dipole magnet. After the first magnet, position sensitive counters and a dipole magnet are located to measure momentum of the particles. In general, a spectrometer for a lower beam energy requires wider aperture of the spectrometer. Since the proposed experiment

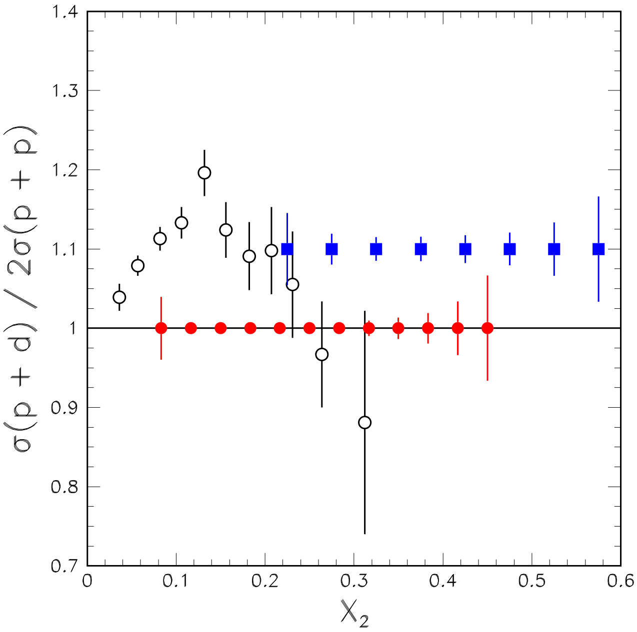

Figure 4: $(p+d)/(p+p)$ Drell-Yan ratios from E866 (open circles) are compared with the expected sensitivities at the 120 GeV Main Injector (solid circles) and the 50-GeV J-PARC (solid squares) of 60-day measurements with the proton and deuterium targets and 1×10^{12} per spill proton beam.

uses 50- and 30-GeV proton beams, a spectrometer for the experiment should have wider aperture than the E906 spectrometer at the main injector with 120-GeV proton beams. But to keep a similar total momentum kick with a realistic magnetic field and to realize the spectrometer with a realistic cost, the magnets of the same size as the E906 spectrometer have been selected, which has a sufficiently large acceptance. Schematic view of the spectrometer are shown in Fig. 5. This magnet can be constructed using a part of iron from existing magnets at Fermilab plus new coils. The design of the copper beam dump including its cooling system and the detailed configuration of the hadron absorber is to be developed. The second magnet has a smaller field integral but a larger aperture.

The 50-GeV proton beam at J-PARC presents an excellent opportunity for extending the $\bar{d}/\bar{u}$ measurement to larger x ($x > 0.25$). For given values of x_1 and x_2 the Drell-Yan cross section at 50 GeV is roughly 16 times greater than that at 800 GeV. Figure 4 shows the expected statistical accuracy for $\sigma(p+d)/2\sigma(p+p)$ at the 50-GeV J-PARC compared with the data from E866 and a proposed measurement using the 120 GeV proton beam at the Fermilab Main-Injector. A definitive measurement of the $\bar{d}/\bar{u}$ over the region $0.25 < x < 0.6$ could be obtained at the 50-GeV J-PARC.

2.2 Flavor Asymmetry of the Sea-Quark Polarization

To restrict the quark and gluon contribution to the nucleon spin with high precision, it is important to know the flavor-sorted sea-quark contribution to the nucleon spin directly.

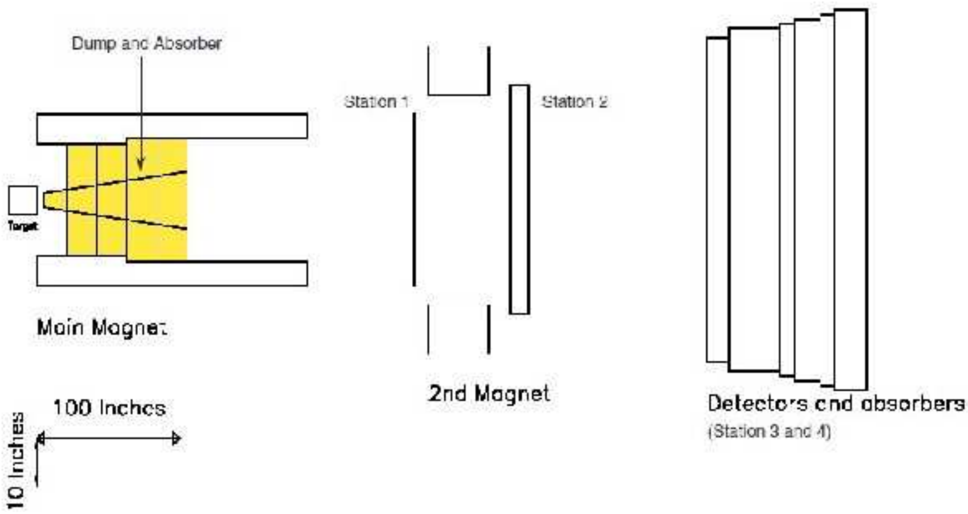

Figure 5: Schematic view of the prototype spectrometer.

Because the Q^2 evolution of the quark and gluon distribution mixes them, uncertainties of the flavor-sorted sea-quark distribution propagate to uncertainties of the quark and gluon distributions. It is also important to know the helicity distribution of the sea-quark at high-x to give an additional input to the physics of the flavor asymmetry of the sea-quark distribution shown in the unpolarized distribution by the Fermilab E866 experiment.

Despite extensive work on polarized DIS, the helicity distributions of $\bar{u}$ and $\bar{d}$ sea quarks are still poorly known. Both the SMC [26] and the HERMES [27] experiments attempted to extract the sea-quark polarizations via semi-inclusive polarized DIS measurements, and the results indicate small sea-quark polarization consistent with zero. Different theoretical models make drastically different predictions. In particular, the meson-cloud models, which successfully describe the unpolarized $\bar{d}/\bar{u}$ asymmetry, predict negligible amount of sea-quark polarization.[28] The chiral-quark soliton model, on the other hand, predicts substantial sea-quark polarization. A striking prediction of the chiral-quark model is the large flavor asymmetry of polarized sea-quark polarization. This model predicts a significantly larger values for $\Delta\bar{u}-\Delta\bar{d}$ than for $\bar{d}-\bar{u}$.[29] This prediction and the GRV94 LO parameterization [30] of $x(\bar{d}-\bar{u})$ are shown in the left panel of Fig. 6.

Polarized proton beam at the 50-GeV J-PARC offer an exciting opportunity for probing sea-quark polarizations. The longitudinal spin asymmetry in the DY process is, in leading order, given by [31],

$$A_{LL}^{DY}(x_1, x_2) = \frac{\sum_a e_a^2[\Delta q_a(x_1)\Delta\bar{q}_a(x_2) + \Delta\bar{q}_a(x_1)\Delta q_a(x_2)]}{\sum_a e_a^2[q_a(x_1)\bar{q}_a(x_2) + \bar{q}_a(x_1)q_a(x_2)]}, \quad (1)$$

with $\Delta q_a \equiv q_a^+ - q_a^-$. The superscripts refer to parton spin projections parallel (+) or antiparallel (−) to the proton's spin projection. The right panel of Fig. 6 shows the x_2 dependence of A_{LL}^{DY}, integrated over the spectrometer acceptance, with calculations using polarized PDF parameterization of G-S (set A and C) [32] and GRSV [10]. The statistical accuracy of such a measurement can well test the predictions of various model. Note that the chiral-quark soliton model predicts a large positive A_{LL}^{DY} not shown in this figure. A comparison of $\vec{p}+\vec{p}$ with $\vec{p}+\vec{d}$ will further determine $\Delta\bar{u}-\Delta\bar{d}$, which provides a direct test of the chiral-quark soliton model's prediction of large $\Delta\bar{u}-\Delta\bar{d}$.

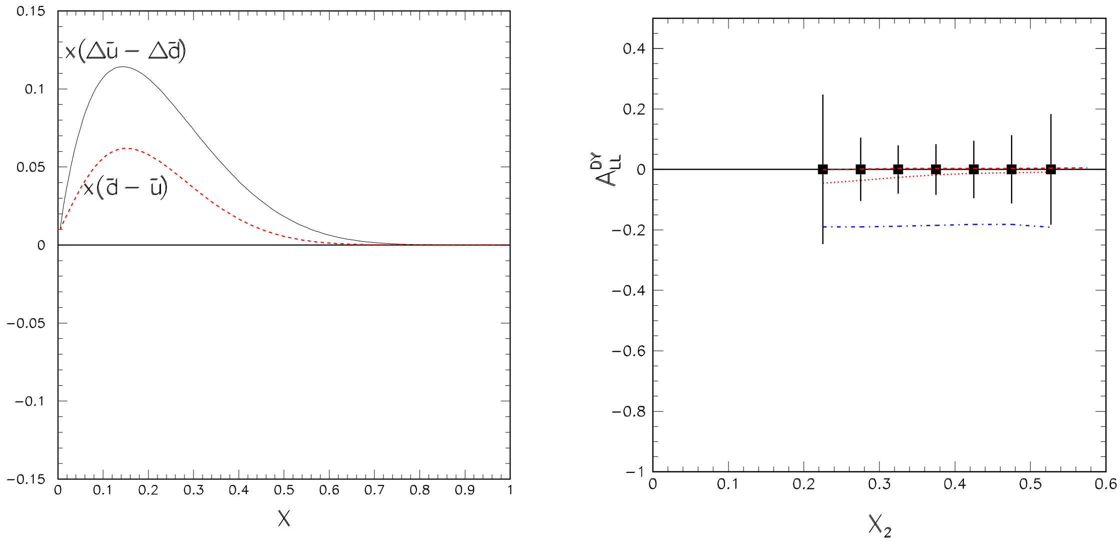

Figure 6: Left: $x(\Delta\bar{u} - \Delta\bar{d})$ predicted by the chiral-quark soliton model is shown as the solid curve. The GRV94 LO parameterization of $x(\bar{d} - \bar{u})$ is shown as the dashed curve. Right: Expected statistical accuracy for measuring A_{LL}^{DY} in polarized $p + p$ Drell-Yan at the 50-GeV J-PARC for a 120-day measurement, assuming 75% polarization for a 5×10^{11} per spill polarized proton beam and a polarized solid NH_3 target of 75% with a dilution factor of 0.15. The dashed, dotted, and dash-dotted curves correspond to calculations using polarized PDF parameterization of G-S (set A and C) and GRSV, respectively. The chiral-quark soliton model gives large positive A_{LL}^{DY}.

Flavor-sorted sea-quark distribution will also be given by the weak-boson measurement at RHIC with 500-GeV polarized-proton collisions in the future (see Fig. 3). While the RHIC experiments will give a $\bar{u}$-quark and $\bar{d}$-quark helicity distribution in the x region of $0.05 - 0.15$, the polarized Drell-Yan measurement at J-PARC will give an flavor asymmetry $\Delta\bar{u} - \Delta\bar{d}$ in the x region of $0.25 - 0.5$. Both measurements are important as complemental data.

2.3 Transverse Single-Spin Asymmetry in Drell-Yan Process

Since we know relatively well the contribution of the quark and gluon to the nucleon spin, and it is not enough to explain the entire contents, we next want to measure the contribution of the orbital angular momentum of the quark and gluon to the nucleon spin as the final object. As a matter of fact, there is no theory model to connect the hadron reaction and the orbital angular momentum contribution to the nucleon spin so far. We will measure the transverse single-spin asymmetry (SSA), or A_N in Drell-Yan process, and explore it.

The Sivers effect and the higher-twist effect generate SSA in Drell-Yan lepton-pair production. Since the Sivers function shows a correlation between the transverse-spin of the nucleon and the transverse momentum of an unpolarized parton inside the nucleon, it contains information of the orbital motion of partons. In Drell-Yan production at

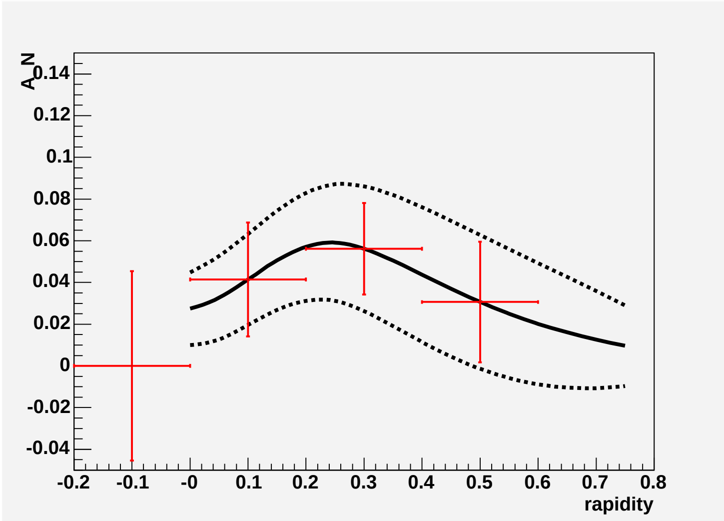

Figure 7: Drell-Yan A_N integrated over q_T of $4 < M_{\mu^+\mu^-} < 5$ GeV at the 50-GeV J-PARC calculated with Sivers function from HERMES data fit. Expected statistical sensitivities for a 120-day measurement are shown.

transverse momentum q_T and pair's mass Q, when q_T, $Q \gg \Lambda_{QCD}$, the higher-twist effect is applicable to calculate A_N. On the other hand, when $q_T \ll Q$, Sivers effect calculation can be applied. In the intermediate region of q_T, $\Lambda_{QCD} \ll q_T \ll Q$, both effects should be applied and yield the same results [19].

It was found that the Sivers function is not universal in hard-scattering reactions, although the non-universality has a clear physical origin. In DIS process, the final-state interaction between the struck parton and the nucleon remnant is attractive. In the Drell-Yan process, it becomes an initial-state interaction and is repulsive. As a result, the Sivers functions contribute with opposite signs to the SSA for these two processes.[22] This is a fundamental QCD prediction, and it tests QCD analysis between $e+p$ reaction and $p+p$ reaction.

Figure 7 shows the A_N integrated over q_T of $4 < M_{\mu^+\mu^-} < 5$ GeV calculated [19, 20] with Sivers function from HERMES data fit [21], and calculated statistical error bars for a 120-day measurement, assuming 75% polarization for a 5×10^{11} per spill polarized proton beam. The experimental condition of this measurement has not been optimized yet and the statistical sensitivity is not good, but it can be much better (e.g. by lowering the lower limit of the invariant mass). First of all, the measurement of the asymmetry sign is very important to verify the QCD prediction.

2.4 Transversity and Boer-Mulders Function

The transversity distribution, $h_1(x)$, is the remaining leading-order polarized distribution function of the nucleon which shows distribution of the transverse-spin of a parton inside the transversely polarized nucleon. The transversity is directly measured only by the double transverse-spin asymmetry A_{TT} in the Drell-Yan production of lepton pairs.[33] It can be accessible by some SSA measurements, but combined with other functions, e.g.

Collins fragmentation function.

$$A_{TT} = \hat{a}_{TT} \cdot \frac{\sum_q e_q^2(\bar{h}_{1q}(x_1)h_{1q}(x_2) + (1 \leftrightarrow 2))}{\sum_q e_q^2(\bar{f}_{1q}(x_1)f_{1q}(x_2) + (1 \leftrightarrow 2))}$$

where

$$\hat{a}_{TT} = \frac{\sin^2\theta\cos(2\phi - \phi_{S_1} - \phi_{S_2})}{1 + \cos^2\theta}$$

and has an azimuthal distribution of $\cos(2\phi - \phi_{S_1} - \phi_{S_2})$. Here, ϕ is an azimuthal angle between the quark-antiquark plane and lepton plane defined in the Collins-Soper frame, and ϕ_{S_1} and ϕ_{S_2} shows an azimuthal angle of the polarization of the hadron with respect to the lepton plane. The transversity distributions are measured as a product of quark's distribution and anti-quark's distribution, $\bar{h}_{1q}(x_1)h_{1q}(x_2)$.

By using either of the transversely polarized beam or target, the $\sin(\phi + \phi_S)$ term of the transverse single-spin measurement gives the transversity distribution combined with the Boer-Mulders function.[34] The Boer-Mulders function, $h_1^{\perp}(x, \boldsymbol{k}_T)$, is a k_T-dependent T-odd PDF which shows a correlation between the transverse-spin and the transverse momentum direction of a parton inside the unpolarized proton. $\boldsymbol{q}_T$ (transverse momentum of virtual photon) weighted single spin asymmetry is defined:

$$\hat{A} \equiv \frac{\int d\Omega d\phi_S \int d^2\boldsymbol{q}_T \frac{|\boldsymbol{q}_T|}{M_p} \sin(\phi + \phi_S)[d\sigma(\boldsymbol{S}_T) - d\sigma(-\boldsymbol{S}_T)]}{\int d\Omega d\phi_S \int d^2\boldsymbol{q}_T [d\sigma(\boldsymbol{S}_T) - d\sigma(-\boldsymbol{S}_T)]}$$

and it gives:

$$\hat{A} = -\frac{1}{2}\frac{\sum_q e_q^2(\bar{h}_{1q}^{\perp(1)}(x_1)h_{1q}(x_2) + (1 \leftrightarrow 2))}{\sum_q e_q^2(\bar{f}_{1q}(x_1)f_{1q}(x_2) + (1 \leftrightarrow 2))}.$$

The Boer-Mulders function are also be measured in the $\sin(2\phi)$ term of the unpolarized Drell-Yan measurement. $\boldsymbol{q}_T$ weighted angular distribution is defined:

$$\hat{R} \equiv \frac{\int d^2\boldsymbol{q}_T \left(\frac{|\boldsymbol{q}_T|}{M_p}\right)^2 \frac{d\sigma^{(0)}}{d\Omega}}{\int d^2\boldsymbol{q}_T \sigma^{(0)}}$$

and parametrized as:

$$\hat{R} = \frac{3}{16\pi}(\gamma(1 + \cos^2\theta) + \hat{k}\cos 2\phi \sin^2\theta).$$

The coefficient $\hat{k}$ at the $\cos 2\phi$-dependent part gives:

$$\hat{k} = 8\frac{\sum_q e_q^2(\bar{h}_{1q}^{\perp(1)}(x_1)h_{1q}^{\perp(1)}(x_2) + (1 \leftrightarrow 2))}{\sum_q e_q^2(\bar{f}_{1q}(x_1)f_{1q}(x_2) + (1 \leftrightarrow 2))}$$

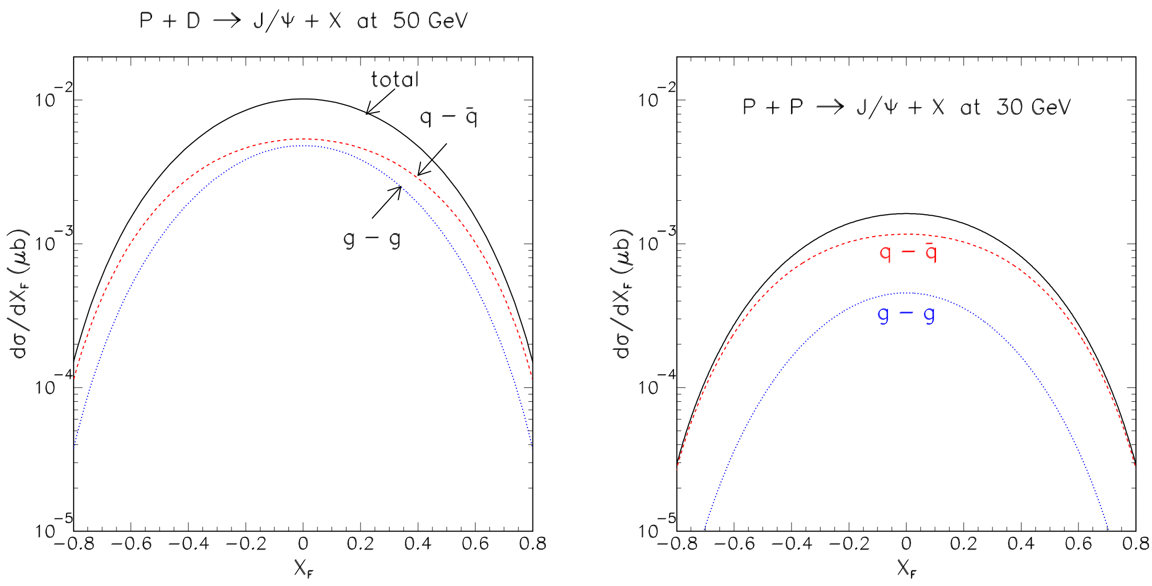

Figure 8: Cross section of the J/ψ production and contribution from the quark-annihilation process (red) and the gluon-fusion process (blue) calculated by the color evaporation model at J-PARC energies: 50 GeV (left) and 30 GeV (right).

where

$$h_{1q}^{\perp(n)} \equiv \int d^2\boldsymbol{k}_T \left(\frac{\boldsymbol{k}_T^2}{2M^2}\right)^n h_{1q}^{\perp}(x, \boldsymbol{k}^2)$$

for the nth moment of the k_T-dependent PDF.

2.5 Spin Physics at 30 GeV

2.5.1 J/ψ Measurement

J/ψ is produced by the gluon-fusion process of quark-annihilation process. At J-PARC energy, it is anticipated that the quark-annihilation process is dominant from the color evaporation model, as shown in Fig. 8. The production mechanism and the dominant process must be determined by measuring its cross section, angular distribution, etc. experimentally. If the J/ψ production is dominated by the quark-annihilation process, we will be able to cover all spin physics topics for the Drell-Yan measurement discussed above by using J/ψ.

2.5.2 Open Charm Measurement

The charm production measured with transversely polarized beam or target also gives us information on the Sivers function. In collider energies, it is dominated by the gluon-fusion process $gg \to c\bar{c}$ and has contributions from the quark-antiquark pair annihilation process $q\bar{q} \to c\bar{c}$ only at the large x_F region. In both processes there is no single spin transfer, so that the final c or $\bar{c}$ quarks are not polarized. Therefore, any SSA observed in the charm production cannot originate from the Collins fragmentation mechanism, but only from the Sivers effect in the distribution function. In particular, any sizable spin

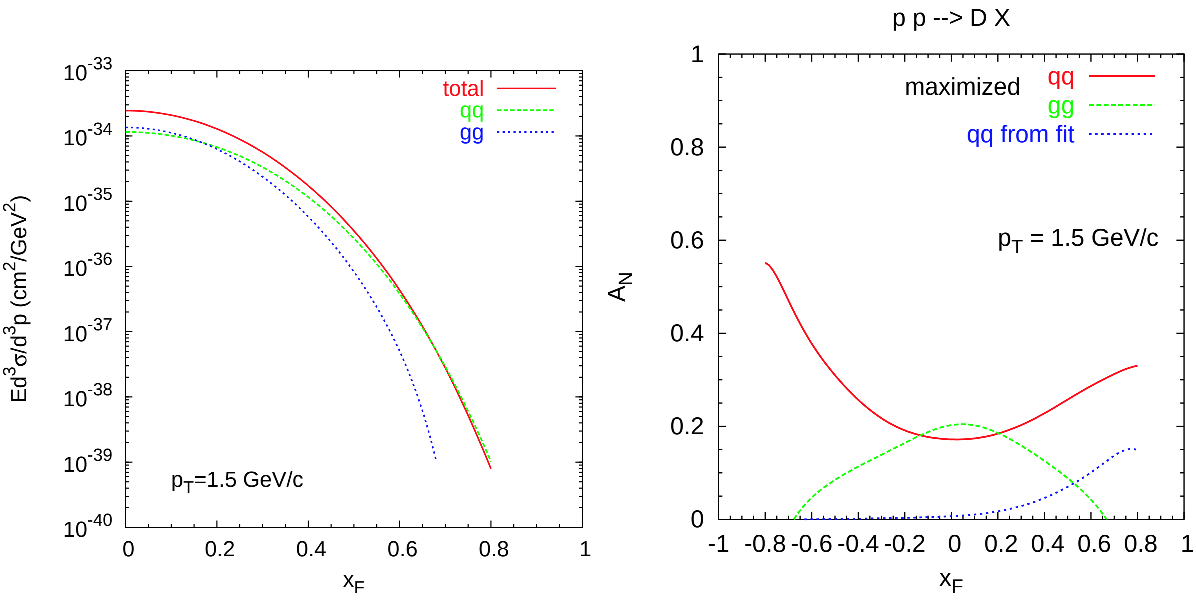

Figure 9: Left: invariant cross section of D-meson production and contributions from both the gluon fusion and quark-antiquark pair annihilation processes on it at the 50-GeV J-PARC. Right: A_N of D-meson production by saturating the Sivers positivity bounds for quarks (maximized qq), for gluons (maximized gg), and by using the parameterizations of the quark Sivers function fit to the E704 data (qq from fit).

asymmetry measured at midrapidity will be a direct indication of a nonzero Sivers gluon distribution function.[23] On the other hand, in J-PARC fixed-target experiment energies, contributions from the gluon-fusion process is much smaller. The SSA measurement is more sensitive to the Sivers quark distribution via the quark-antiquark pair annihilation process. The measurement is complimentary to the collider-energy measurements. Figure 9 shows a x_F spectrum of invariant cross section and A_N of D-meson production and contributions from both the gluon fusion and quark-antiquark pair annihilation processes on it.[24]

2.6 A_N and A_{NN} in elastic scattering

These measurements are proposed by the SPIN@J-PARC collaboration.[25] The goal of these measurements is to determine if the large unexpected value of A_N, discovered in proton-proton elastic scattering at the BNL/AGS, persists to higher energy and higher $P_\perp^2$. This large unexpected spin effect has been difficult to reconcile with most current models of strong interactions, such as perturbative QCD. The validity of perturbative QCD is predicted to improve with increasing energy and increasing $P_\perp^2$.

2.7 Detector issues

As the E906 experiment has been approved and funded at the Fermilab, the major part of the J-PARC experiment can be constructed using the components of the E906 experiment after their completion in 2011. A plan is that the E906 apparatus will be moved

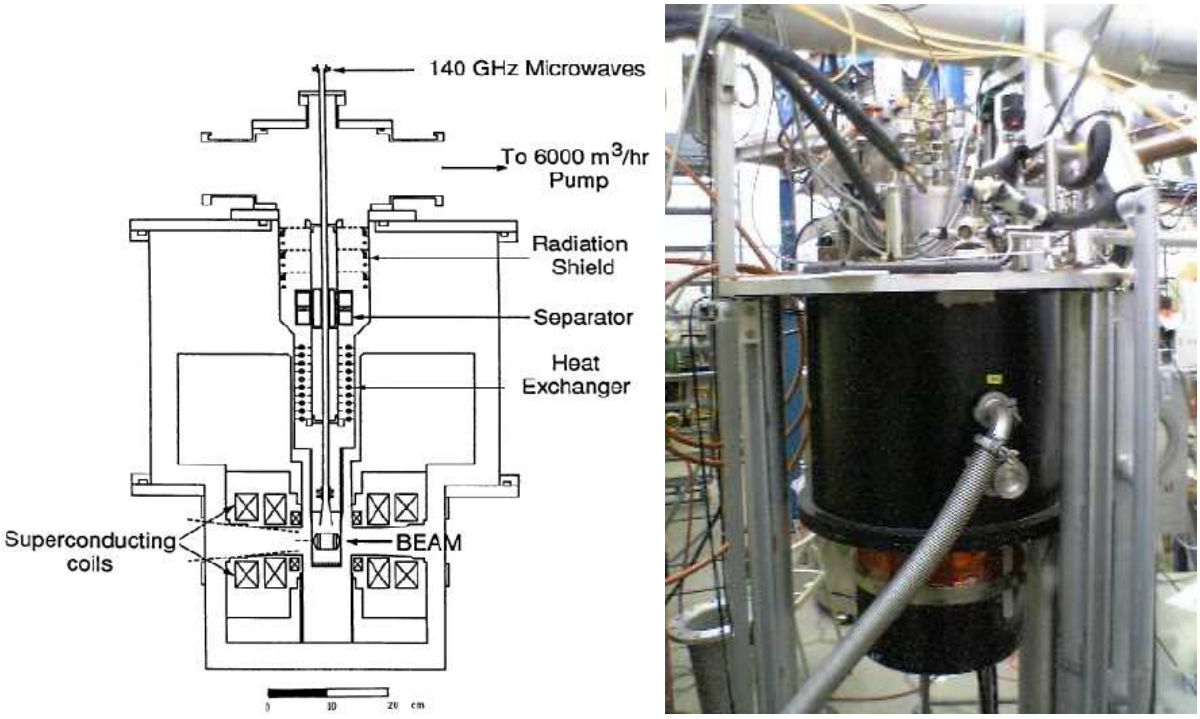

Figure 10: Diagram and picture of the Michigan polarized-proton target. The superconducting magnet produces a highly uniform 5 T field. At 1 K, the ^4He cryostat provides about 1 watt of cooling power to the irradiated 2-mm-diameter NH_3 beads in the small cavity at the field's center. A horn feeds the 140 GHz microwaves, from a 22 watt Varian EIO, into the cavity.

from Fermilab to J-PARC from the summer of 2011, then the experimental setup of this experiment will be prepare in 2011 and 2012.

The difference of the beam energy between 120 GeV and 50 (30) GeV results in a smaller acceptance of muon pairs if one assumes the same setup, since the opening angle of the two muons from a pair is roughly proportional to the inverse of the Lorentz factor γ ($\tan\theta \sim 1/\gamma$). Thus the magnets and the detectors will be relocated so that the total length of the spectrometer becomes shorter from 24 m to 16 m.

2.8 Polarized target

For a final goal of our polarized Drell-Yan experiment, a polarized target which can be used with a beam intensity of 10^{12} protons per sec and has a thickness of 5% interaction length is ideal. Like the SMC polarized target [36], the target volume should be divided to have opposite directions simultaneously, and can have both longitudinal and transverse polarization. There is no such a polarized target in the world due to a heat load issue, etc. The SMC target was used only with a beam intensity of 4×10^7 muons per spill. We need a research and development to get the ideal polarized target.

There is one polarized target (Michigan polarized-proton target) at KEK on a 5-year loan, and may be available at J-PARC experiments.[37] It is a 1-watt-cooling-power polarized proton target which was originally developed and built by University of Michigan group [38], and used at AGS in 1990s.[39] Figure 10 shows its diagram. Its magnetic field of 5 T and temperature of 1 K produced a high proton polarization of up to 96%. Its 5-minute polarization rise-time allowed fast and frequent polarization-direction reversals. The target's material is 2 mm beads of radiation-doped ammonia (NH_3), with a hydrogen density of about 0.10 g/cm^3. Its length is about 3.2 cm, and its diameter is 2 cm. The H protons in the NH_3 are polarized in the 5 T field, by a 140 GHz microwave system, using the Dynamic Nuclear Polarization method and some nearby electrons in radiation-damage centers. The polarization is monitored by a 213 MHz NMR Q-meter system. This polarized target had an average polarization of 85% at AGS, with an average beam intensity of about 10^{11} protons per sec.

This polarized-proton target can be used for low-luminosity test experiment, and also development of a larger target with higher cooling performance. To improve the cooling performance, a basic development item is a shape of the target material, radiation-doped NH_3. In order to make the surface area as wide as possible, the shape of the solid NH_3 can be made e.g. powdered state, porous beads, or layer-stack films.

3 Polarized proton acceleration

3.1 Modes of operation

To meet the requirements of spin physics program, operation modes of the J-PARC Main Ring should be:

- 50 GeV maximum energy
- 10^{12} proton/spill ($\sim 10^{36}$/cm^2/sec luminosity with a $\sim$5% interaction target)
- spin length 0.5 sec (working assumption)
- 80% polarization
- normalized emittance 10 π mm mrad 95%

3.2 Polarized ion source

The required polarized beam intensity of about 2×10^{11} p/RCS bunch can be produced in the Optically-Pumped Polarized H^- Ion Source (OPPIS) similar to the RHIC source. To meet the requirements of spin physics program the J-PARC Main Ring (MR – 50 GeV maximum energy) should deliver about 10^{12} p/spill. With the 8 bunches in MR this required RCS bunch intensity will be about 1.5×10^{11} p/bunch and polarized source intensity of about 5×10^{11} H^-/source pulse (in assumption of about 50% beam losses in LEBT, RFQ, Linac and further 40% losses in RCS). Therefore the following OPPIS parameters for J-PARC polarized operation will be required:

- Peak current 0.16 mA
- Pulse duration 500 μs
- Repetition rate 50 Hz

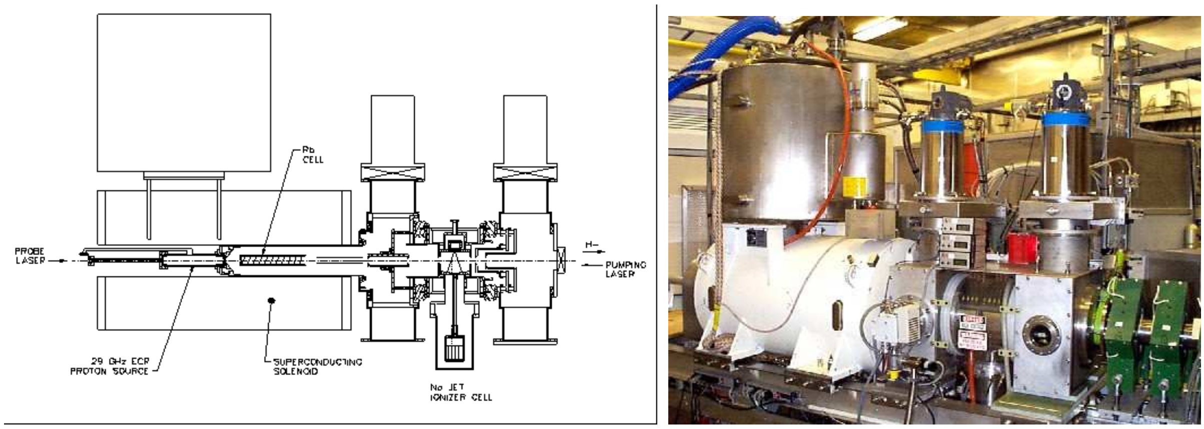

Figure 11: RHIC OPPIS general layout and picture.

- Normalized emittance 1.0 π mm mrad
- Beam energy 35 keV
- Polarization 85%

The RHIC OPPIS produces 0.5-1.0 mA (maximum 1.6 mA) H^- ion current in a 400 μs pulse (which corresponds to $1.2 - 2.4 \times 10^{12}$ H^-/pulse) with the maximum repetition rate of a 7 Hz (routine repetition rate is 1 Hz) and polarization 82-85%.[40] The OPPIS technique is based on spin-transfer proton (or atomic hydrogen) collisions in an optically-pumped alkali metal cell. The modern technology involved – a superconducting solenoid, a 29.2 GHz microwave generator, and high power solid state tunable lasers – is essential to the OPPIS technique. In the BNL OPPIS, an ECR-type source produces a primary proton beam of a 2.0 – 3.0 keV energy, which is converted to electron-spin polarized H atoms by electron pick-up in an optically pumped Rb vapor cell. A pulsed Cr:LISAF laser of a 1 kW peak at 500 μs pulse duration is used for optical pumping. The nuclearly polarized H atoms are then negatively ionized in a Na-jet vapor cell to form nuclear polarized H^- ions.

The ECR primary proton source in the RHIC OPPIS is operated in dc mode, producing a dc H^- ion beam (see Fig. 11). Pulsed 35 keV beam is produced by accelerating voltage pulse applied to sodium-jet ionizer cell. At 7 Hz repetition rate it was operated reliably and with the latest improvements implemented to reduce possible HV discharge current in ionizer the 50 Hz operation is feasible. The required beam intensity 0.16 mA cab be obtained also in dc operation by using dc lasers for optical pumping as it was demonstrated in the TRIUMF OPPIS.[41] Then 50 Hz repetition rate is not a problem. Pulsed laser application as in the RHIC OPPIS will not require continuous 50 Hz laser pulsing but only 8 pulses over 320 ms period every 3 seconds for injection to MR. This will require some laser system upgrade, perhaps using two lasers tuned for opposite spin state wavelength operated in sequence at 25 Hz repetition rate.

There is also an option of splitting one linac pulse to two bunches in RCS. This will be also a benefit for longitudinal emittance reduction. The required doubling of the source intensity is not a problem. In this case the laser repetition rate will be 12.5 Hz which probably can be obtained by minor RHIC OPPIS laser system upgrade.

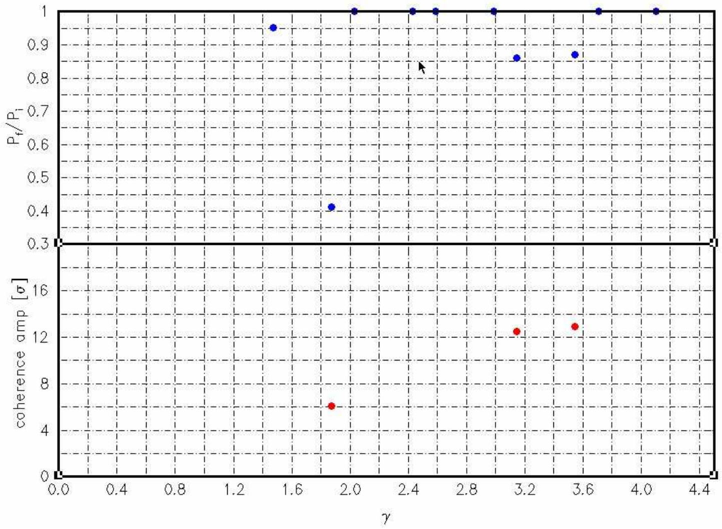

Figure 12: Intrinsic spin resonance spectrum for RCS. The bottom figure shows a required amplitude of the coherent oscillation by the rf dipole to achieve more than 99% spin flip.

The ECR-based OPPIS can be upgraded with atomic hydrogen injector to produce 50 mA polarized H^- ion beam.[42] This would be a great benefit for the polarized program because it can be run in parallel with the other experiments. In present acceleration scheme the polarized beam intensity will be limited by rf dipole operation in RCS, probably at the level of $1-2\times10^{11}$ p/bunch. The rf dipole can be also upgraded to partial helical snakes. The OPPIS with atomic hydrogen injector can also produce the unpolarized H^- ion beam with much greater brightness than volume type source. This can be used for the future J-PARC intensity upgrade.

We need a discussion of where to locate the polarized ion source and how to merge the polarized beam to the existing beam line. Maintenance issue of the laser system needs to be considered.

3.3 From source to RCS

At the end of the linac, we need a polarimeter. This polarimeter can be a proton-Carbon elastic scattering polarimeter similar to that in the BNL facility. It measures a left-right asymmetry of charged particles.

There is a 300–500 μg/cm^2 stripping foil for injection to RCS. This may need to be replaced by 100 μg/cm^2 stripping foil to have better dp/p.

3.4 Accelerating polarized protons in the RCS

The kinetic energy of the RCS spans from .18 to 3 GeV ($G\gamma$ =2.2 to 7.5). The five imperfection resonances can easily be corrected by harmonic orbit correction. With the periodicity 3 and a vertical tune ν_y of 6.35 there are four intrinsic resonances in this range: $9-\nu_y$, $-3+\nu_y$,$12-\nu_y$, and $0+\nu_y$. As shown in Fig. 12, simulations showed that the latter three resonances are strong enough so that a modest 20 Gm vertical rf dipole can produce enough coherence to cause complete spin flip. Quite large coherence can be produce in

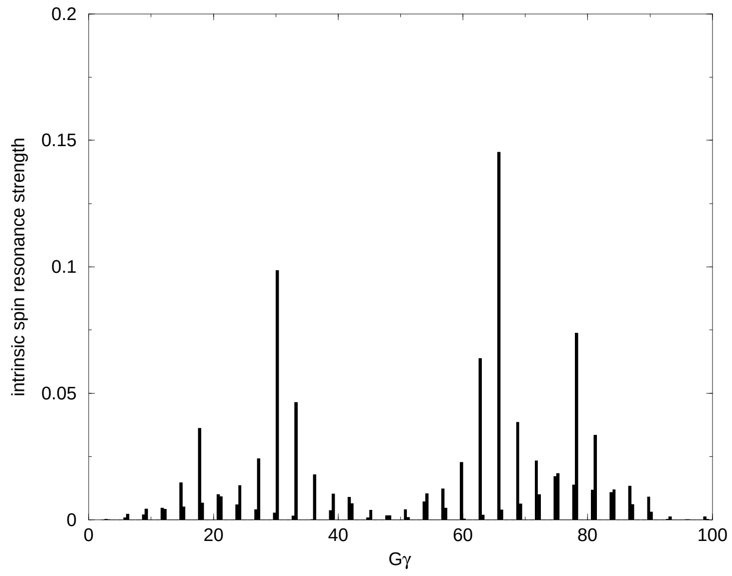

Figure 13: Intrinsic spin resonance spectrum for MR.

the RCS because of the very large available aperture in this high intensity synchrotron. In order to design the rf dipole magnet, 7cm size of the painting beam will require 95-cm gap of the magnet from the required 13-σ amplitude of the coherence oscillation to achieve more than 99% spin flip. This is too big and it is hard to achieve a good enough uniform field of this size. We need to consider painting beam scheme for the polarized beam. The first intrinsic resonance is too week for this technique. However, with the fast repetition rate of 25 Hz the depolarization is only 5%.

We need a discussion where to locate the rf dipole. Another discussion item is a beam monitor system which can cover a wide dynamic range between high-intensity unpolarized beam (4×10^{13}/bunch) and polarized beam (1.5×10^{11}/bunch).

3.5 Accelerating polarized protons in the MR

The main ring [43], designed to accelerate protons from 3 to 50 GeV ($G\gamma$ =7.5 to 97.5) at a tune ν_x=22.339, ν_y=20.270, exhibits many imperfection and strong intrinsic spin resonances, Fig. 13. Its lattice is compact and offers no space to insert full Siberian snakes. Available straight sections for snakes are only able to accommodate partial snakes of the type used in the AGS [44, 45].

A solution is obtained by using two 30% partial snakes separated by 120^0 in beam deflection as shown in Fig. 1. Fig. 14, shows the theoretical vertical component of the stable spin axis and the spin tune with two such snakes. The working betatron tunes should be chosen in the two gaps near an integer tune value and the vertical tune needs to be close to an integer that is a multiple of 3.

Using the tunes 22.128 and 20.960, Fig. 15 shows the results of spin tracking of a beam of 12 particles of emittance $4\pi\mu$m (1.5σ), with two partial snakes. Essentially no polarization is lost during acceleration in the MR.

As shown in Fig. 16, the J-PARC MR has 3 superperiods, each with an insertion: INSA, INSB and INSC. We have selected two drift sections 3 m long in INSA and INSB,

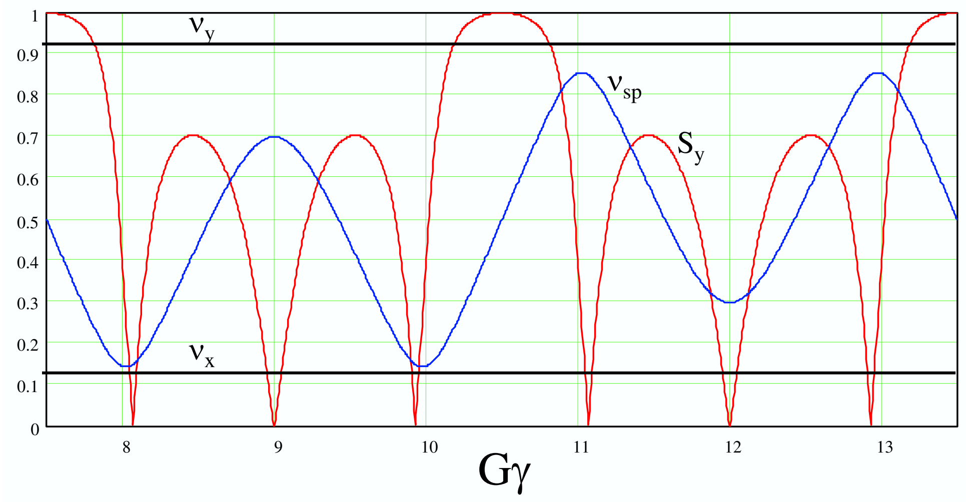

Figure 14: Spin tune ν_{sp} and vertical component of the stable spin direction S_y as a function of $G\gamma$ for two 30% partial snakes in the J-PARC MR. $\nu_x = 22.12$ and $\nu_y = 20.96$ are placed between the spin tune and the integer.

between the injection and slow extraction, where AGS type helical snakes can be placed. Scaling from the AGS, a 30% snake at injection for the MR could be obtained with a field $B = 3.4$ Tesla. The dual pitch helical dipole design of the AGS partial snakes [46] does not affect the beam orbit direction. However, it focuses in both planes. The focusing decreases with beam energy and increases with B as $B^2/(\beta\gamma)^2$. Because of the strong focusing of the snakes, they produce a substantial perturbation of the lattice at low energies. This can be compensated with two quadrupole doublets on either sides of each snake [48]. We studied a solution using the existing quadrupole type QDT, QFP, QFT and QFS, that only needs 4 additional power supplies. Required correcting quadrupole strengths decrease as $1/(\beta\gamma)^2)$ during acceleration. Fig.17(L) shows the matching result at $\gamma = 11$.

Snake focusing at injection may not allow both horizontal and vertical tunes to be so close to an integer. However, since the spin depolarization resonances in the MR at low energy are very weak, and the amount of depolarization is negligible, we are allowed to ramp the two betatron tunes to near integer starting from values more separated from the integers. A possible tune path is shown in Fig. 17(R).

Figure 18 shows a picture of the superconducting partial helical snake magnet built at BNL.

Design issues of the snake magnet are e.g. orbital distortion, correction scheme for imperfection resonances, etc.

3.6 Primary beam extraction

Although we don't expect any serious issue in the primary beam extraction, we will study effects on polarization in the extraction, tune change for the extraction, vertical bent of the beam line, etc. We need a spin rotator magnet to manipulate a direction of beam polarization, and a beam profile monitor system for the stability of beam intensity, position, and spot size to provide a systematical control of the experimental data quality.

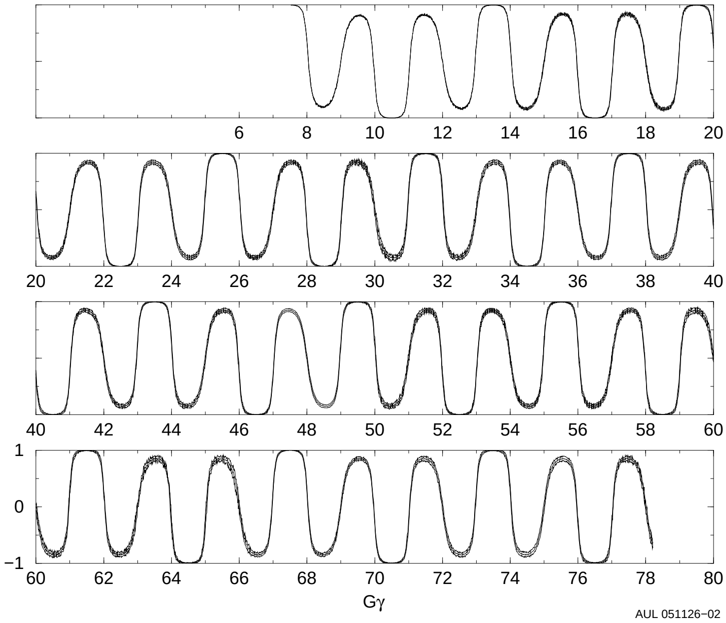

Figure 15: Spin tracking of a bunch of particles at 1.5σ with two 30% snakes. The average vertical spin $< S_y > \pm\sigma$ is shown.

3.7 Polarimeter

3.7.1 proton-Carbon elastic-scattering polarimeter

At BNL, proton-Carbon elastic-scattering polarimeters in the Coulomb Nuclear Interference region (CNI polarimeter) were built and installed at AGS and RHIC. These CNI polarimeters detect recoil carbons by Si strip detectors and identify the elastic scattering by kinematics cuts. Figure 19 shows a picture of the CNI polarimeter at RHIC. The CNI polarimeter with a recoil-carbon detection technique provide a quick turn-around to optimize machine parameters to achieve maximum polarization with a low cost. This technique is applicable to J-PARC with some optimizations and developments of readout electronics, radiation damage of sensors and electronics, and thin carbon targets. We need a discussion where to locate the polarimeters and how to insert carbon targets.

3.7.2 absolute polarimeter

There is a measured analyzing power data of the *pp* and *pC* elastic scattering at 31.2 GeV of the RHIC beam. This data can be used as a reference point, and used for calibration of absolute polarimeter of the main ring (gas jet) and extracted beam (solid target).

4 Cost

A rough cost estimation for the polarized proton acceleration at J-PARC which is mainly based on the cost of BNL facility is summarize on Table 1.

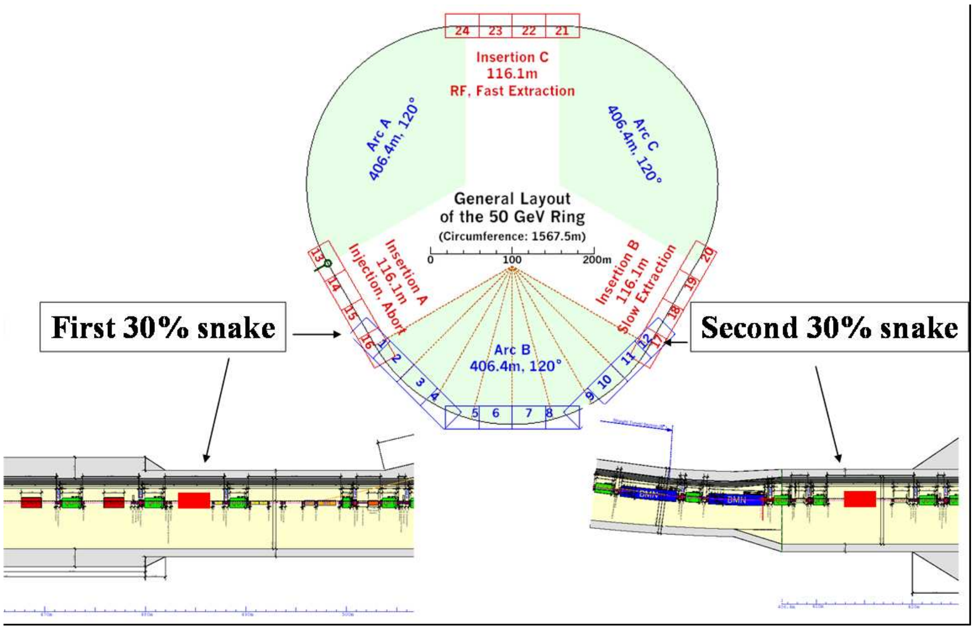

Figure 16: Possible location of partial helical snake magnets in the MR.

Item	Cost (million yen)
Polarized ion source	200
Source to RCS	50
Polarization in RCS	100
Polarized beam in MR	500
Primary beam extraction	250
pC polarimeter	100
Absolute polarimeter	100 - 300
Total	1,300 - 1,500

Table 1: Rough cost estimation for the polarized proton acceleration at J-PARC.

5 Summary

We propose to make the J-PARC facility allow acceleration of polarized proton beams to 30-50 GeV for experiments using this primary beam. We have studied the feasibility of polarized proton acceleration at J-PARC consisting of a 400 MeV linac, a 3 GeV rapid cycling synchrotron (RCS) and a 50 GeV synchrotron (MR). We show how the polarization of the beam can be preserved using an rf dipole in the RCS and two superconducting partial helical Siberian snakes in the MR. As a main physics case, polarized Drell-Yan measurement by the dimuon experiment will provide us flavor asymmetry of the sea-quark polarization, Sivers function, Transversity and Boer-Mulders function to understand the polarized proton structure.

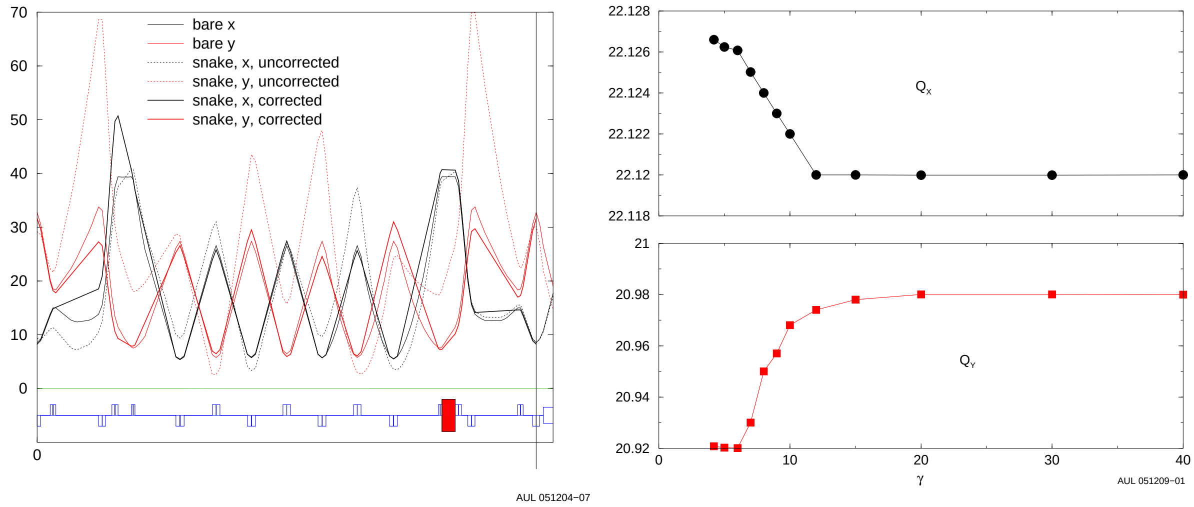

Figure 17: (**L**) Matching of the INSA with snake at the energy $\gamma = 11$. (**R**) Tune path used in the matching of snakes to MR.

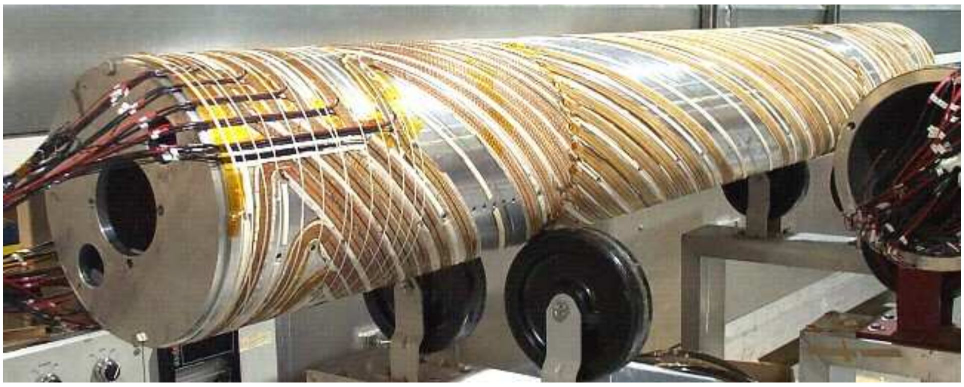

Figure 18: Picture of a completed helical dipole coil of the superconducting partial helical snake magnet built at BNL.

References

[1] A.U.Luccio *et al.*, SPIN2006, AIP Conf. Proc. 915, p.944.

[2] H. Huang et al., "Acceleration of polarized protons in the AGS with two helical partial snakes", Proceedings of EPAC2006, Edinburgh, Scotland, p. 273

[3] H. Huang *et al.*, Phys. Rev. Lett. **99**, 154801 (2007).

[4] J.-C. Peng, S. Sawada *et al.*, Proposal "Measurement of High-Mass Dimuon Production at the 50-GeV Proton Synchrotron", April 2006: Addendum to the Proposal, June 2007.

[5] J. Ashman *et al.*, Phys. Lett. B **206**, 364 (1988).

[6] B. Adeva *et al.*, Phys. Rev. D **58**, 112002 (1998).

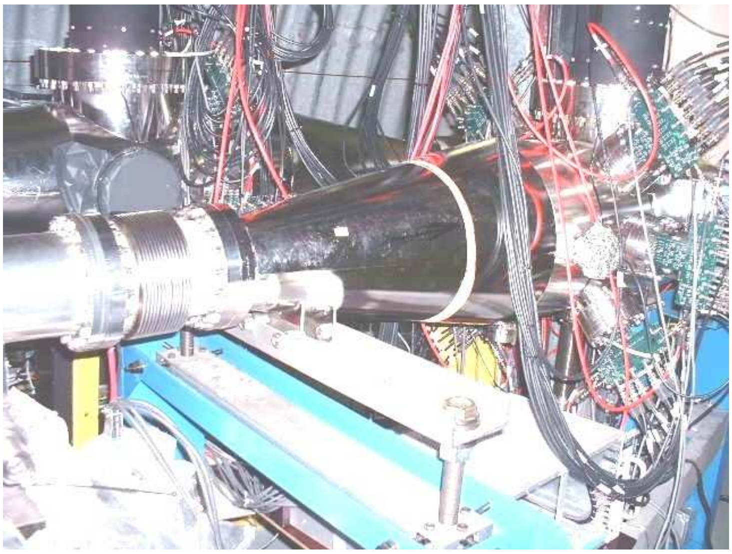

Figure 19: Picture of a CNI polarimeter at RHIC.

[7] P. L. Anthony *et al.*, Phys. Lett. B **493**, 19 (2000).

[8] E. S. Ageev *et al.*, Phys. Lett. B **633**, 25 (2006).

[9] A. Airapetian *et al.*, Phys. Rev. Lett. **84**, 2584 (2000).

[10] M. Glück, E. Reya, M. Stratmann and W. Vogelsang, Phys. Rev. D **53**, 4775 (1996).

[11] B. Jager, A. Schafer, M. Stratmann and W. Vogelsang, Phys. Rev. D **67**, 054005 (2003).

[12] K. Boyle, AIP Conf. Proc. **842**, 351 (2006) [arXiv:nucl-ex/0606008]: S. S. Adler *et al.*, Phys. Rev. D **73**, 091102 (2006): Phys. Rev. Lett. **93**, 202002 (2004).

[13] B. I. Abelev *et al.*, submitted to Phys. Rev. Lett. [arXiv:hep-ex/0608030].

[14] D. L. Adams *et al.*, Phys. Lett. B **261**, 201 (1991): Phys. Lett. B **264**, 462 (1991).

[15] J. C. Collins, Nucl. Phys. B **396**, 161 (1993).

[16] D. W. Sivers, Phys. Rev. D **41**, 83 (1990).

[17] J. Qiu and G. Sterman, Phys. Rev. D **59**, 014004 (1999).

[18] E. A. Hawker *et al.*, Phys. Rev. Lett. **80**, 3715 (1998).

[19] X. Ji, J. Qiu, W. Vogelsang and F. Yuan, Phys. Rev. Lett. **97**, 082002 (2006): Phys. Rev. D **73**, 094017 (2006).

[20] F. Yuan and W. Vogelsang, private communications.

[21] W. Vogelsang and F. Yuan, Phys. Rev. D **72**, 054028 (2005).

[22] J. C. Collins, Phys. Lett. B **536**, 43 (2002).

[23] M. Anselmino, M. Boglione, U. D'Alesio, E. Leader and F. Murgia, Phys. Rev. D **70**, 074025 (2004).

[24] U. D'Alesio, private communications.

[25] A. D. Krisch *et al.*, SPIN@J-PARC Proposal "Analyzing power A_n and A_{nn} in 30-50 GeV very-high-$P_\perp^2$ proton-proton scattering", November 2007.

[26] B. Adeva *et al.*, Phys. Lett. B **420**, 180 (1998).

[27] K. Ackerstaff *et al.*, Phys. Lett. B **464**, 123 (1999).

[28] K. G. Boreskov and A. B. Kaidalov, Eur. Phys. J. C **10**, 143 (1999): R. J. Fries and A. Schafer, Phys. Lett. B **443**, 40 (1998).

[29] K. Goeke, P. V. Pobylitsa, M. V. Polyakov and D. Urbano, Nucl. Phys. A **680**, 308 (2001).

[30] M. Gluck, E. Reya and A. Vogt, Z. Phys. C **67**, 433 (1995).

[31] F. E. Close and D. Sivers, Phys. Rev. Lett. **39**, 1116 (1977).

[32] T. Gehrmann and W. J. Stirling, Phys. Rev. D **53**, 6100 (1996).

[33] V. Barone, A. Drago and P. G. Ratcliffe, Phys. Rept. **359**, 1 (2002).

[34] A. N. Sissakian, O. Y. Shevchenko, A. P. Nagaytsev and O. N. Ivanov, Phys. Rev. D **72**, 054027 (2005).

[35] R. L. Jaffe and D. Kharzeev, Phys. Lett. B **455**, 306 (1999).

[36] D. Adams *et al.*, Phys. Lett. B **329**, 399 (1994).

[37] S. Ishimoto and H. M. Shimizu, private communication.

[38] D. G. Crabb *et al.*, Phys. Rev. Lett. **64**, 2627 (1990).

[39] D. G. Crabb *et al.*, Phys. Rev. Lett. **65**, 3241 (1990).

[40] A. Zelenski *et al.*, Rev. Sci. Instr. **73**, 888 (2002).

[41] A. Zelenski, SPIN2000, AIP Conf. Proc. 570, 187 (2000).

[42] A. Zelenski, to be published in Proc. of SPIN2006 conference.

[43] JAERI/KEK JointProjectTeam, Accelerator Technical Design Report for J-PARC, KEK Report 2002-13, JAERI-Tech 2003-044, J-PARC 03-01, March 2003, A

[44] A.U.Luccio,R.Gupta,W.MacKay, and T.Roser, Report C-A/AP/128, December 2003.

[45] A.U.Luccio, "Tracking of polarized protons in the Main Ring of the J-PARC accelerator facility", KEK Report 2005-11, January 2006.

[46] E. Willen et al., "Superconducting helical snake magnet for the AGS", Proceedings of PAC2005, Knoxville, Tennessee, p. 2935

[47] A.U.Luccio, in "Trends in Collider Spin Physics", World Scientific, 1995, p.235

[48] E.D.Courant, SPIN2002, AIP Conf. Proc. 675, p.799